A nonlinear piezoelectric energy harvester with magnetic oscillator

Tang, Lihua; Yang, Yaowen

2012

Tang, L., & Yang, Y. (2012). A nonlinear piezoelectric energy harvester with magnetic oscillator. Applied Physics Letters, 101(9), 094102-.

https://hdl.handle.net/10356/95117

https://doi.org/10.1063/1.4748794

AIP | Applied Physics Letters

A nonlinear piezoelectric energy harvester with magnetic oscillator

Lihua Tang and Yaowen Yang

Citation: Appl. Phys. Lett. **101**, 094102 (2012); doi: 10.1063/1.4748794
View online: http://dx.doi.org/10.1063/1.4748794
View Table of Contents: http://apl.aip.org/resource/1/APPLAB/v101/i9
Published by the American Institute of Physics.

Related Articles

Nonlinear output properties of cantilever driving low frequency piezoelectric energy harvester
Appl. Phys. Lett. 101, 223503 (2012)

A review on frequency tuning methods for piezoelectric energy harvesting systems
J. Renewable Sustainable Energy 4, 062703 (2012)

Effects of ocean thermal energy conversion systems on near and far field seawater properties—A case study for Hawaii
J. Renewable Sustainable Energy 4, 063104 (2012)

Limit on converted power in resonant electrostatic vibration energy harvesters
Appl. Phys. Lett. 101, 173904 (2012)

Metamaterial particles for electromagnetic energy harvesting
Appl. Phys. Lett. 101, 173903 (2012)

Additional information on Appl. Phys. Lett.

Journal Homepage: http://apl.aip.org/
Journal Information: http://apl.aip.org/about/about_the_journal
Top downloads: http://apl.aip.org/features/most_downloaded
Information for Authors: http://apl.aip.org/authors

ADVERTISEMENT

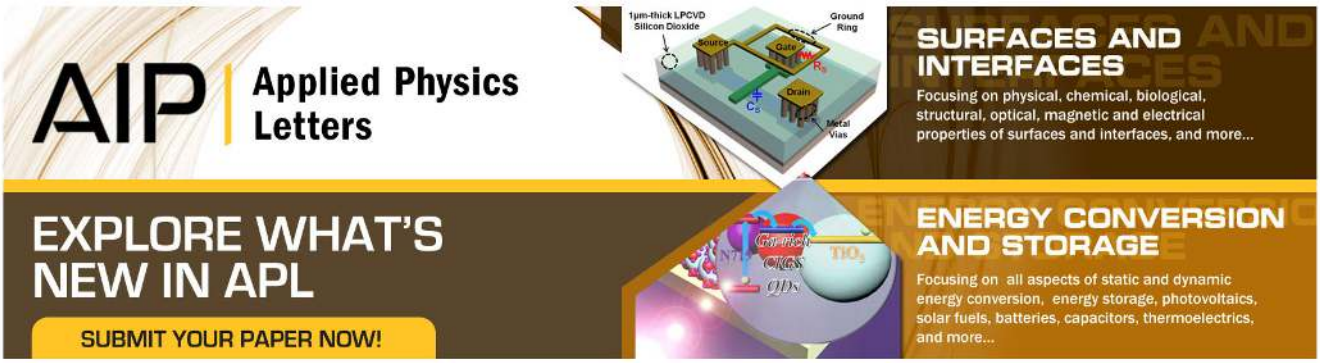

A nonlinear piezoelectric energy harvester with magnetic oscillator

Lihua Tang and Yaowen Yang[a)]
School of Civil and Environmental Engineering, Nanyang Technological University, 50 Nanyang Avenue, Singapore 639798

(Received 24 June 2012; accepted 15 August 2012; published online 27 August 2012)

This letter proposes a magnetic coupled piezoelectric energy harvester (PEH), in which the magnetic interaction is introduced by a magnetic oscillator. For comparison purpose, lumped parameter models are established for the conventional linear PEH, the nonlinear PEH with a fixed magnet, and the proposed PEH with a magnetic oscillator. Both experiment and simulation show the benefits from the dynamics of the magnetic oscillator. In the experiment, nearly 100% increase in the operating bandwidth and 41% increase in the magnitude of the power output are achieved at an excitation level of 2 m/s^2. © *2012 American Institute of Physics*. [http://dx.doi.org/10.1063/1.4748794]

Vibration energy harvesting provides a promising solution to implement self-sustained lower-power electronic devices and hence has attracted numerous research interests.[1–5] The efforts to improve the efficiency of a vibration energy harvester (VEH) involve both enlarging the magnitude of output and widening the operating bandwidth. Multimodal energy harvesting is one strategy widely pursued for broadband purpose.[6–11] The conventional cantilever configuration of VEHs can provide multiple resonances, however, high-order vibration modes are usually useless, since they are far away from the fundamental mode and have much smaller magnitudes.[6,7] Though some specific two degree-of-freedom (DOF) VEH configurations can be tuned to have two close modes,[9–11] they fail to outperform the conventional single DOF harvester in terms of the maximum achievable output. Magnetic interaction has also been frequently adopted for broadband energy harvesting.[12–22] The magnets can be used to tune the resonant frequency of a VEH to adaptively match the excitation frequency.[12,13] However, the energy used for detecting frequency change and automatic tuning will consume a great amount of harvested energy.[13] The magnet interaction also introduces the nonlinearity to the system other than the linear stiffness change. Mann and Sims[15] presented a design for electromagnetic energy harvesting from the hardening nonlinear oscillations of magnetic levitation, which covered an useful range of 8–13 Hz when excited at 4 m/s^2. Stanton *et al.*[16] proposed a monostable piezoelectric energy harvester (PEH) in which both the hardening and softening responses could occur by tuning the magnetic interactions. A broad operational bandwidth of 14–24 Hz was obtained at a high acceleration of 0.5 g. Erturk *et al.*[17] reported a bistable piezomagnetoelastic energy harvester under sinusoidal excitation. Other researchers[14,18–22] studied the performance of bistable structures employing magnets under random vibrations. At sufficiently large excitation (e.g., 0.35 g in Ref. 17), these bistable configurations could have remarkable improvement in performances with high-energy attractors at off-resonance frequencies and thus achieve broad bandwidths. For the above nonlinear designs, however, no obvious superiority to conventional linear VEH was observed at low-level excitations. One common feature of these reported energy harvesters is that they interact with the magnets fixed at the enclosure of the device.

This Letter reports a magnetic coupled PEH to achieve both wide bandwidth and enhanced output power at relatively low excitation by introducing a magnetic oscillator. A typical PEH is usually designed as a cantilever beam with piezoelectric element bonded at the root and a proof mass at the free end (Figure 1(a)). By replacing the proof mass with a magnet and fixing another magnet at the enclosure of the device (Figure 1(b)), the resonant frequency of the PEH can be altered by tuning the distance between the magnets. For such configuration, nonlinear behavior appears when the harvester is subjected to high-level excitations. We propose to replace the fixed magnet at the enclosure with a movable magnetic oscillator, i.e., an additional magnetic mass-spring-damper subsystem, as depicted in Figure 1(c). The dynamics of the magnetic oscillator affects the behavior of the PEH in a more complex way other than introducing the hardening or softening nonlinear stiffness to the PEH.

For a conventional linear cantilever PEH subjected to base motion $u_0(t)$, we only concern the response near the fundamental mode and the vibratory motion of the beam relative to the base can be expressed as $w(x,t) = \phi(x)\eta(t)$. The single-mode governing equations are expressed as

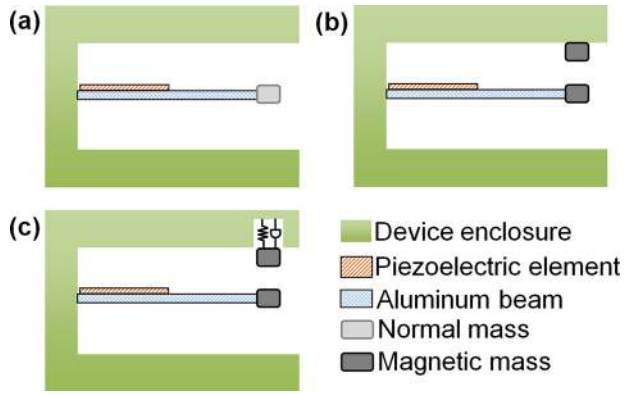

FIG. 1. Various PEH configurations: (a) Linear PEH; (b) Nonlinear PEH interacting with fixed magnet at enclosure; (c) Proposed nonlinear PEH interacting with magnetic oscillator.

[a)]Author to whom correspondence should be addressed. Electronic mail: cywyang@ntu.edu.sg.

$$\begin{cases} \ddot{\eta}(t) + 2\zeta\omega_n\dot{\eta}(t) + \omega_n^2\eta(t) + \chi V(t) = -\left[\int_0^L m(x)\phi(x)dx + M_t\phi(L)\right]\ddot{u}_0(t) = -f\ddot{u}_0(t) \\ I(t) + C^S\dot{V}(t) - \chi\dot{\eta}(t) = 0 \end{cases}, \tag{1}$$

where $\phi(x)$, $\eta(t)$, ω_n, ζ, and f are the mode shape function, modal coordinate, natural frequency, damping ratio, and forcing coefficient, respectively; χ is the modal electromechanical coupling coefficient; L, $m(x)$, and M_t are the length, mass per length, and proof mass of the cantilever beam, respectively; $V(t)$ and $I(t)$ are the voltage and current outputs from the PEH, respectively; and C^S is the clamped capacitance of the piezoelectric transducer. The displacement at the tip is $u(t) = w(L, t) = \phi(L)\eta(t)$. Letting $M_{eq} = 1/\phi^2(L)$, $C_{eq} = 2\zeta\omega_n/\phi^2(L)$, $K_{eq} = \omega_n^2/\phi^2(L)$, and $\Theta = \chi/\phi(L)$, and considering a resistive load R, Eq. (1) is rearranged as

$$\begin{cases} M_{eq}\ddot{u}(t) + C_{eq}\dot{u}(t) + K_{eq}u(t) + \Theta V(t) = -\mu M_{eq}\ddot{u}_0(t) \\ V(t)/R + C^S\dot{V}(t) - \Theta\dot{u}(t) = 0 \end{cases}. \tag{2}$$

This is the lumped parameter model of the linear PEH, where M_{eq}, C_{eq}, and K_{eq} are the equivalent mass, damping, and stiffness of the PEH, respectively; and $\mu = f\phi(L)$ is the correction factor of forcing function.[2]

In the case that the PEH interacts with a magnet fixed at the enclosure of the device, we assume a magnetic dipole-dipole interaction[16] between the magnetic proof mass and the fixed magnet. In addition, we assume that the directions of the magnetic dipoles are always vertically aligned during the vibrations of the PEH. Based on these assumptions, the magnetic force is expressed as

$$F_{mag} = -\frac{3\tau m_1 m_2}{2\pi\left(u(t) + D_0\right)^4}, \tag{3}$$

where m_1 and m_2 are the moments of the magnetic dipoles; τ is the vacuum permeability; and D_0 is the initial distance between the magnetic dipoles. For attractive magnets, $m_1 = -m_2$, while for repulsive magnets, $m_1 = m_2$. Adding F_{mag} into the left hand side of Eq. (2) forms the electromechanically coupled governing equations of the nonlinear PEH with a fixed magnet.

Subsequently, we replace the fixed magnet at the enclosure with a magnetic oscillator, which has the parameters of M_{eq2}, C_{eq2}, K_{eq2}, and μ_2. The notations for the parameters of the PEH are modified by adding the subscript 1. Again, we assume that the magnetic dipoles are vertically aligned with a dipole-dipole interaction. The magnetic force is then modified as

$$F_{mag} = -\frac{3\tau m_1 m_2}{2\pi\left(u_1(t) - u_2(t) + D_0\right)^4}. \tag{4}$$

The electromechanically coupled lumped parameter model of the system is described as

$$\begin{cases} M_{eq1}\ddot{u}_1(t) + C_{eq1}\dot{u}_1(t) + K_{eq1}u_1(t) + \Theta V(t) - \dfrac{3\tau m_1 m_2}{2\pi\left(u_1(t) - u_2(t) + D_0\right)^4} = -\mu_1 M_{eq1}\ddot{u}_0(t) \\ M_{eq2}\ddot{u}_2(t) + C_{eq2}\dot{u}_2(t) + K_{eq2}u_2(t) + \dfrac{3\tau m_1 m_2}{2\pi\left(u_1(t) - u_2(t) + D_0\right)^4} = -\mu_2 M_{eq2}\ddot{u}_0(t) \\ V(t)/R + C^S\dot{V}(t) - \Theta\dot{u}_1(t) = 0 \end{cases}. \tag{5}$$

Equation (5) can be further written in the state space form and the system dynamics can be simulated by numerical integration.

A prototype of the proposed nonlinear PEH with magnetic oscillator is devised (Figure 2(a)). The entire experiment setup is shown in Figure 2(b). The device comprises two aluminum cantilever beams with magnetic proof masses. The top one with a strain gauge serves as a magnetic oscillator. The bottom one is bonded with a piezoelectric macro fiber composite (MFC) (Smart Materials Corp., model: M2807-P2) at its root, serving as a PEH. The MFC weighs 0.38 g and has a clamped capacitance C^S of 11.45 nF. The aluminum beams have the same dimension of 70*10*0.6 mm^3 and weight of 1.134 g. The proof masses (including the magnet and plastic holder) attached on the top and bottom cantilevers weigh 5.9 g and 4.52 g, respectively, and their centers are exactly located at the free end of the cantilevers. Two NdFeB cylinder magnets embedded in the proof masses are spanned around 10 mm and have the same diameter of 4 mm, thickness of 3 mm, and surface flux of 3200 gauss. They are regarded as two magnetic dipoles with the effective magnetic moment m of 0.0192 Am^2. If the top cantilever is replaced with a much stiffer one (e.g., 2 mm in thickness), it can be regarded as a fixed magnet at the enclosure. If the top cantilever is removed, the system degrades to a conventional linear PEH.

Prior to the simulation and model validation, the system parameters should be determined from experiment. The

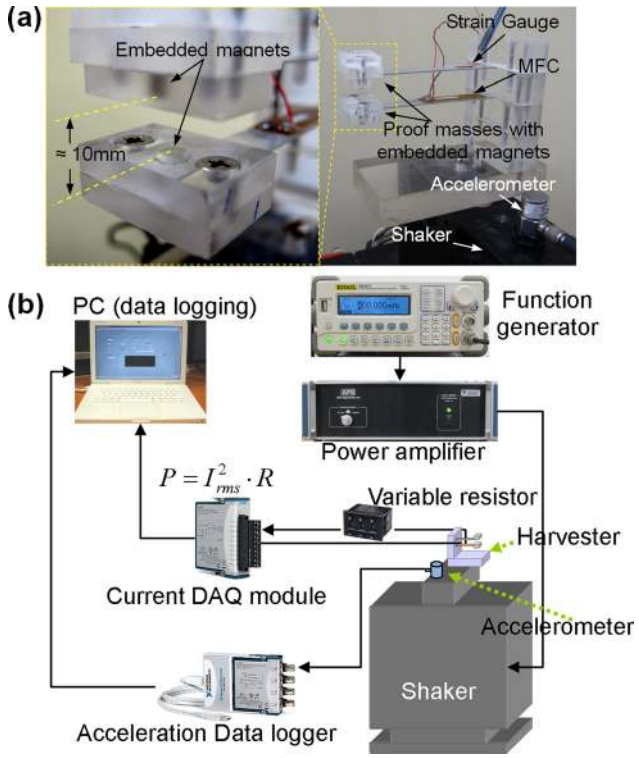

FIG. 2. (a) Prototype of nonlinear PEH with magnetic oscillator and (b) Entire experiment setup.

magnetic oscillator and PEH are tested separately at this stage. M_{eq} can be approximated by $M_{eq} = (33/140)M_b + M_t$, where M_b is the distributed mass of a cantilever. The resonant frequencies of the magnetic oscillator and PEH can be determined by measuring the strain and the short circuit current I_{sc}, respectively, and thus K_{eq} can be calculated. In addition, ζ and C_{eq} are determined by the log decrement method from the attenuation curves of the strain of the magnetic oscillator and the I_{sc} of the PEH. μ can be calculated by referring to Ref. 2. The last undetermined parameter is the coupling coefficient Θ of the PEH. χ has the relation with I_{sc} at unity root mean square acceleration (a_{RMS}) at resonance as $f = 2\zeta\omega_n I_{sc}(\omega_n)/\chi$.[23] Considering $\mu M_{eq} = f/\phi(L)$, $C_{eq} = 2\zeta\omega_n/\phi^2(L)$, and $\Theta = \chi/\phi(L)$, we can determine $\Theta = C_{eq} I_{sc}(\omega_n)/(\mu M_{eq})$. All the system parameters are identified as shown in Table I.

Optimal power is the major concern when we evaluate the performance of a PEH. In the experiment, we note that although the optimal resistive load varies with frequency, the system performance has very minor difference near the optimal load at a specific frequency. It is found that the optimal power or near optimal power is achieved with a resistor of 400 kΩ in the widest concerned range near resonance. Hereafter, the results and discussion of experiment and simulation are based on the power with the resistive load of 400 kΩ.

TABLE I. Identified system parameters.

Parameters	Magnetic oscillator	PEH
M_{eq} (g)	6.167	4.877
K_{eq} (Nm^{-1})	144.9	148.8
C_{eq} (Nsm^{-1})	0.0178	0.01534
Θ (NV^{-1})	—	1.71×10^{-4}
$I_{sc}(\omega_n)$ (μA)	—	56.5
μ	1.026	1.04
C^S (nF)	—	11.45

We conduct frequency sweep under two excitation levels ($a_{RMS} = 1\,m/s^2$ and $2\,m/s^2$) for different harvester configurations. For the linear PEH, the power at resonance from simulation (360 μW, Figure 3(d)) is close to the experimental result (322 μW, Figure 3(a)) under low excitation ($a_{RMS} = 1\,m/s^2$). However, simulation predicts larger response (1440 μW) than that obtained in experiment (1015 μW) with the increased excitation ($a_{RMS} = 2\,m/s^2$). The discrepancy may result from the fact that the damping changes with the vibration level and frequency in the experiment but a constant damping ratio is used in the simulation. In the nonlinear PEH with fixed magnet, the two embedded magnets are arranged in the attractive way. Under low excitation level ($a_{RMS} = 1\,m/s^2$), the PEH still behaves like a linear one but the resonance is slightly shifted to the left. With the increase of excitation ($a_{RMS} = 2\,m/s^2$), weak nonlinear response is observed in both experiment and simulation by upward sweep and downward sweep (Figures 3(b) and 3(e)). It is believed that stronger nonlinear response can be expected if the excitation level is further increased.[15] However, compared to the linear PEH, the fixed magnet brings no benefit and even reduces the magnitude of the achieved power.

Figures 3(c) and 3(f) depict the response of the nonlinear PEH with an attractive magnetic oscillator from experiment

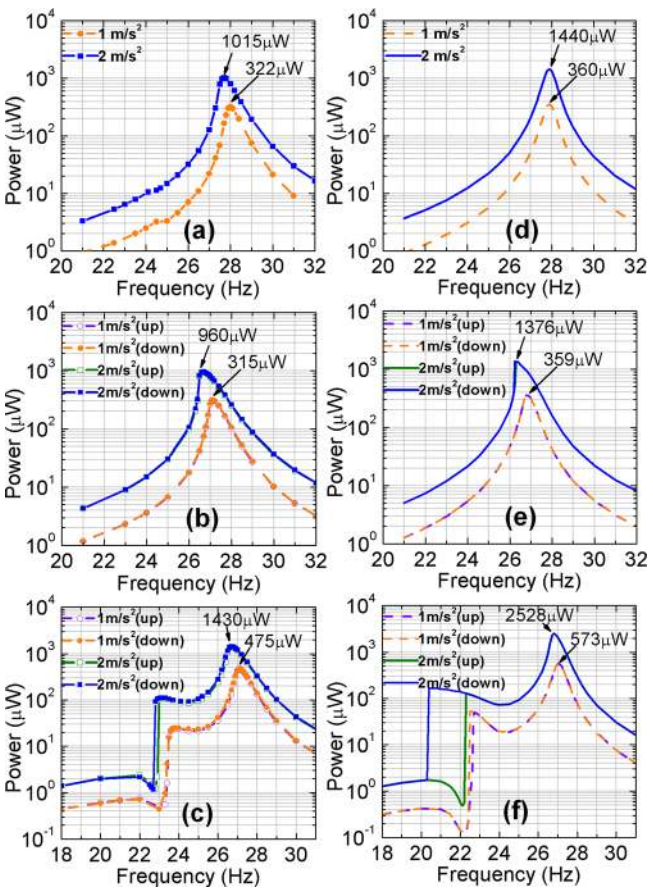

FIG. 3. Power from various configurations. (a) and (d) Linear PEH; (b) and (e) Nonlinear PEH with fixed magnet; (c) and (f) Nonlinear PEH with magnetic oscillator. (a)~(c) Experiment; and (d)~(f) Simulation.

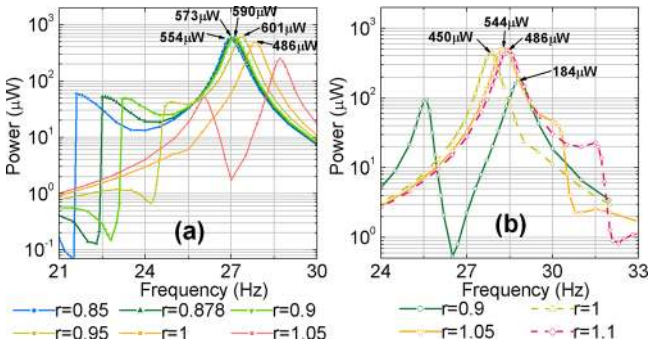

FIG. 4. Power from various configurations at $a_{RMS} = 1 m/s^2$ by simulation. (a) Attractive and (b) repulsive magnetic oscillators.

and simulation. At the power level of 100μW (required by a wireless sensor[5]), the proposed PEH with magnetic oscillator at $a_{RMS} = 2\,m/s^2$ provides a bandwidth of 6 Hz (Figure 3(c)), which is more than 100% wider than those provided by the linear PEH and the PEH with a fixed magnet (less than 3 Hz in Figures 3(a) and 3(b)). In addition, the maximum power achieved by the proposed PEH at $a_{RMS} = 2\,m/s^2$ is 1430 μW (Figure 3(c)), corresponding to 41% and 49% increase as compared to those achieved by its counterparts (1015 μW, Figure 3(a) and 960 μW, Figure 3(b)). The reason for the improved performance of the system can be attributed to the involved dynamics of the magnetic oscillator. When we sweep the frequency near the resonances of the magnetic oscillator (24.4 Hz) or the PEH (27.8 Hz), the vibration energy of the magnetic oscillator is partially transferred to the PEH via magnetic interaction to enhance its output. Furthermore, it is worth mentioning that with the increase of excitation ($a_{RMS} = 2\,m/s^2$), the discrepancy between the experiment and simulation lies in two aspects. First, more remarkable difference in the magnitude of power near resonance is observed. Besides the difference of damping in the experiment and simulation, this discrepancy also results from the assumption that the magnetic dipoles are always vertically aligned. This assumption becomes inappropriate when the PEH and magnetic oscillator undergo large oscillations where the rotations at the free ends of the two cantilevers are no longer negligible and may be of different values. Due to the fact that the magnetic oscillator further improves the vibration of the PEH, it is understandable that the discrepancy is more pronounced. Second, it is observed in Figures 3(c) and 3(f) that the effective response from the simulation can be extended further by downward sweep and the multivalued response range is much broader than those obtained in the experiment. Again, the alignment assumption of magnetic dipoles overestimates such nonlinear behavior of the proposed PEH. These discrepancies become small at low excitation level ($a_{RMS} = 1\,m/s^2$). In general, the simulation predicts the same trends of nonlinear behaviors of the proposed PEH as the experiment, that is, the proposed PEH can provide a much wider bandwidth as well as a significantly enhance the achievable power.

To have a complete picture of the influence of the magnetic oscillator, both attractive and repulsive magnetic oscillators are considered in simulation. A parameter study on $r = \omega_{n2}/\omega_{n1}$ is conducted, where ω_{n1} and ω_{n2} are, respectively, the resonant frequencies of the PEH and the magnetic oscillator when they work separately. Downward sweep for attractive oscillators and upward sweep for repulsive oscillators are conducted at $a_{RMS} = 1\,m/s^2$ (Figure 4). By comparing Figures 4 and 3(d), we note the significant improvement in power magnitude with $r < 1$ (but close to 1) for attractive oscillators and with $r > 1$ (but close to 1) for repulsive oscillators. It is also noted in Figure 4 that certain tradeoff is required between the magnitude of power output and the broad bandwidth.

In summary, this Letter reports a nonlinear PEH with a magnetic oscillator. The lumped parameter model of such system is presented. Both experiment and simulation show that the introduction of the magnetic oscillator can broaden the operating bandwidth and at the same time substantially enhance the achievable power.

[1]S. R. Anton and H. A. Sodano, Smart Mater. Struct. **16**, R1 (2007).
[2]A. Erturk and D. J. Inman, Smart Mater. Struct. **17**, 065016 (2008).
[3]D. P. Arnold, IEEE Trans. Magn. **43**, 3940 (2007).
[4]Y. W. Yang, L. H. Tang, and H. Y. Li, Smart Mater. Struct. **18**, 115025 (2009).
[5]L. H. Tang, Y. W. Yang, and C. K. Soh, J. Intell. Mater. Syst. Struct. **21**, 1867 (2010).
[6]Q. Ou, X. Q. Chen, S. Gutschmidt, A. Wood, N. Leigh, and A. F. Arrieta, J. Intell. Mater. Syst. Struct. **23**, 117 (2012).
[7]M. Arafa, W. Akl, A. Aladwani, O. Aldrarihem, and A. Baz, Proc. SPIE **7977**, 79770Q (2011).
[8]A. Erturk, J. M. Renno, and D. J. Inman, J. Intell. Mater. Syst. Struct. **20**, 529 (2009).
[9]H. Wu, L. H. Tang, Y. W. Yang, and C. K. Soh, Jpn. J. Appl. Phys., Part 1 **51**, 040211 (2012).
[10]I.-H. Kim, H.-J. Jung, B. M. Lee, and S.-J. Jang, Appl. Phys. Lett. **98**, 214102 (2011).
[11]L. H. Tang and Y. W. Yang, J. Intell. Mater. Syst. Struct. **23**, 1627 (2012).
[12]V. R. Challa, M. G. Prasad, Y. Shi, and F. T. Fisher, Smart Mater. Struct. **17**, 015035 (2008).
[13]D. Zhu, S. Roberts, J. Tudor, and S. Beeby, "Closed Loop Frequency Tuning of a Vibration-based Micro-generator," Proc. PowerMEMS 229 (2008).
[14]L. H. Tang, Y. W. Yang, and C. K. Soh, J. Intell. Mater. Syst. Struct. **23**, 1431 (2012).
[15]B. P. Mann and N. D. Sims, J. Sound Vib. **319**, 515 (2009).
[16]S. C. Stanton, C. C. McGehee, and B. P. Mann, Appl. Phys. Lett. **95**, 174103 (2009).
[17]A. Erturk, J. Hoffmann, and D. J. Inman, Appl. Phys. Lett. **94**, 254102 (2009).
[18]F. Cottone, H. Vocca, and L. Gammaitoni, Phys. Rev. Lett. **102**, 080601 (2009).
[19]S. C. Stanton, C. C. McGehee, and B. P. Mann, Physica D **239**, 640 (2010).
[20]M. Ferrari, V. Ferrari, M. Guizzetti, B. Andò, S. Baglio, and C. Trigona, Sens. Actuators A **162**, 425 (2010).
[21]J. Lin and B. Alphenaar, J. Intell. Mater. Syst. Struct. **21**, 1337 (2010).
[22]B. Andò, S. Baglio, C. Trigona, N. Dumas, L. Latorre, and P. Nouet, J. Micromech. Microeng. **20**, 125020 (2010).
[23]Y. W. Yang and L. H. Tang, J. Intell. Mater. Syst. Struct. **20**, 2223 (2009).